Polymer Degradation and Stability 154 (2018) 203–210

Contents lists available at ScienceDirect

Polymer Degradation and Stability

journal homepage: www.elsevier.com/locate/polydegstab

UV degradation model for polymers and polymer matrix composites

T. Lu, E. Solis-Ramos, Y. Yi, M. Kumosa*

National Science Foundation Industry/University Cooperative Research Center for Novel High Voltage/Temperature Materials and Structures, University of Denver, 2155 E Wesley Ave, Denver, 80208, USA

ARTICLE INFO

Article history:
Received 21 March 2018
Received in revised form
21 May 2018
Accepted 9 June 2018

Keywords:
UV radiation damage
Modeling
Polymers
PMCs

ABSTRACT

We are proposing in this work a new model of ultraviolet (UV) damage for polymers and Polymer Matrix Composites (PMCs). Flat and sinusoidal polymer surfaces were numerically simulated for their UV damage as a function of UV intensity, surface topography, and exposure time. Experimentally determined UV degradation rates for a unidirectional glass/epoxy composite were used to predict numerically the local rates of material degradation on sinusoidal epoxy surfaces subjected to UV. This allowed us to show that UV damage on uneven polymer surfaces reduces their surface roughness making them planar and that the degradation rates are the largest at the tips of the local heights of the surfaces. This was subsequently verified experimentally by exposing neat epoxy specimens to UV in air at 80 °C for 1000 h and by precisely monitoring their surface topography as a function of time. It was found that the surface roughness of the epoxy was reduced by about 12.5% and that UV affected the local peaks on the surfaces of the specimens more than the valleys.

© 2018 Published by Elsevier Ltd.

1. Introduction

Severe exposure to UV radiation can rapidly accelerate degradation processes in polymeric materials [1–20]. UV radiation causes photooxidative aging, which results in the breakage of polymer chains, produces free radicals and reduces the molecular weight of polymers, resulting in a loss of surface gloss and the significant deterioration of many material properties with time. Extensive research has been performed on systematic experimental evaluations of degradations mechanisms in polymer coatings, polymer resins and Polymer Matrix Composites (PMCs) after long-term artificial UV exposures [1–20]. However, few studies have concentrated specifically on the development of analytical models of UV aging of polymeric materials [7–12].

For a polymer subjected to UV radiation, photodegradation is the main damage mechanism. Photodegradation initiates with the absorption of UV photons by chromophores i.e. hydroperoxides, catalyst residues, carbonyls, and unsaturated molecules containing double and triple bonds, and/or rings [13]. The activation processes initiated by UV photons excite states in macromolecules which leads to surface discoloration, yellowing and a loss of surface gloss [14,15]. Further exposure to UV light results in the formation of a thin layer consisting of loosely adherent particles called chalking [1,16–18]. Depending on the type of a polymer, flaking of surface resin, pitting and microcracking may also occur [6,19]. In addition, chemical aging such as chain scission by UV will result in a loss of low molecular weight or highly volatile products, which can vaporize very quickly at elevated temperature [13,20].

Most current environmental aging models for polymers and PMCs are limited to one individual degradation factor such as UV light, elevated temperature, water diffusion and others [21–26]. Few studies have concentrated on synergistic aging under multiple aging conditions involving UV [1,2,27–31]. It was shown, for example in Refs. [1,2], that the combined cyclic UV-temperature-moisture conditions resulted in severe damage to the polymer matrices of several different PMCs, and that the damage under the cyclic conditions was more severe than under consecutive but non-cyclic UV and water conditions. It has also been concluded in Ref. 1 that UV alone can damage PMC surfaces by a formation of microparticles, as shown in Fig. 1a, and that the process rapidly accelerates if slow moving water is present on the surface of the composites for debris removal purposes (Fig. 1b). Without the involvement of water, however, the particles formed by UV tend to stay on the surfaces and prevent further development and progression of UV degradation of the undelaying virgin material [1,2]. At the same time water alone does not cause much degradation in comparison with UV [1,28]. The strong UV/water condensation aging of the composites observed in Ref. [1] has been recently

* Corresponding author.
E-mail address: Maciej.Kumosa@du.edu (M. Kumosa).

https://doi.org/10.1016/j.polymdegradstab.2018.06.004
0141-3910/© 2018 Published by Elsevier Ltd.

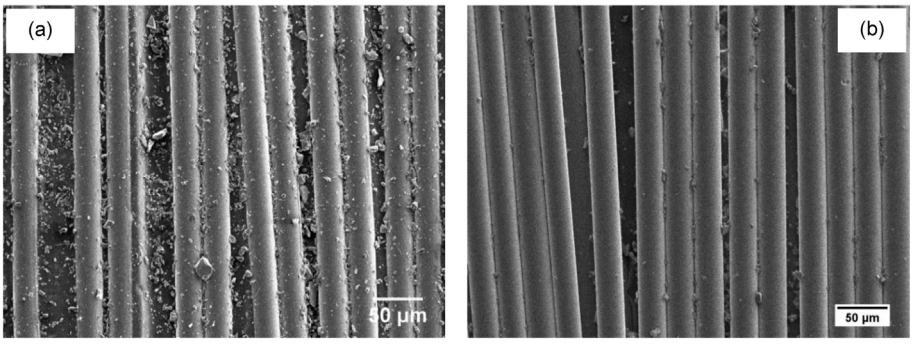

Fig. 1. SEM images of unidirectional ECR-glass/epoxy composite; a) after UV radiation and b) after cyclic UV & moisture condensation [1].

supported by a comprehensive particle removal model [2].

In this work, we are suggesting another model, which could further contribute to our understanding of the synergistic aging process of polymers involving UV. In particular, we are showing (1) how to properly simulate UV damage on wavy polymer surfaces typical for unidirectional composites, (2) how to predict UV degradation rates of polymers, in general, and (3) how the surface topographies of polymers change with time under UV exposure.

2. Fundamentals of our UV degradation model

In this study, the degradation mechanisms on polymeric surfaces exposed to UV were investigated with the assumptions that the air temperature, humidity and UV radiation intensity were all constant. It was also assumed that the modeled polymer surfaces were free from photon stabilizers, antioxidants, or other additives, and that the contributions from individual wavelengths were independent, also neglecting reflections of the parallel UV light. Only a fraction of absorbed photons led to photolytic activity, and the photo recovery effect was neglected. The UV radiation intensity received by simulated material surfaces corresponded to the UV tests performed in Ref. 1. Also, no thermal degradation was incorporated and the initial surface profiles were either flat or sinusoidal (sin (x)).

Photodegradation of polymeric surfaces by radiation fields can be estimated by using the cumulative damage model, which has been widely accepted in medical and biological studies [31]. Here, an approximate function of the total effective dosage is given by equation (1) according to the accumulative dosage model [10,32].

$$D_{total}(t) = \int_0^{\tilde{t}} \int_{\lambda_{min}}^{\lambda_{max}} E_o(\lambda, t)\left(1 - e^{-A(\lambda)}\right)\phi(\lambda)d\lambda dt \tag{1}$$

where: $\lambda_{\min}$ and λ_{max} are the minimum and maximum photolytically effective wavelengths (nm). $A(\lambda)$ is the absorbance of the sample at specified UV wavelength, (dimensionless). $E_o(\lambda)$ is the incident spectral UV radiation dose to which a polymeric material is exposed to (W m^{-2}). $\phi(\lambda)$ is the quantum yield, which is the number of times a specific event occurs per photon absorbed by the material. The "event" is typically a kind of chemical reaction, (dimensionless). t is the elapsed time and $\tilde{t}$ is the total radiation time (in seconds). D_{total} (t) is the total effective dosage (J m^{-2}).

It is assumed here that there is no UV radiation transmitted through the sample. By the Lambert-Beer law (equation (2)) [31], we find that $A(\lambda)$ is infinitely large if $I(\lambda)$ is close to zero.

$$In\left(\frac{I_o(\lambda)}{I(\lambda)}\right) = A(\lambda) \tag{2}$$

where $I_o(\lambda)$ is the irradiance of the incident light at wavelength λ, $I(\lambda)$ is the intensity of the transmitted light at wavelength λ, and $A(\lambda)$ is the absorbance at wavelength λ. Therefore, the probability of absorption of UV photons by a material is 1 ($e^{-A(\lambda)} \approx 0$). We can simplify the total effective dosage function by (3).

$$D_{total}(t) = \int_0^{\tilde{t}} \int_{\lambda_{min}}^{\lambda_{max}} E_o(\lambda, t)\phi(\lambda)d\lambda dt \tag{3}$$

According to Martin et al. [32], different incident wavelengths have different quantum efficiencies.

It is assumed in this research that the only photosentitive group in the aromatic epoxy network is phenoxy which only absorbs in the interval 300–340 nm and that the quantum efficiency for this effective absorbed wavelength is 10^{-4} [26]. Equation (3) can then be simplified further into equation (4).

$$D_{total}(t) = E_o \times \phi \times t \tag{4}$$

In most cases there is an angle between the incident light and the sample surface [33]. The intensity of irradiation is therefore determined by equation (5), where I_o is the intensity of UV light (W/m^2•s) and θ is the angle between the UV light and the normal to the surface.

$$E_o = I_o(\lambda, \theta, t)\cos(\theta) \tag{5}$$

The relationships between UV damage to polymeric materials and the radiation dosages can be approximated by a linear response (equation (6)), a power law response (equation (7)), or by an exponential response (equation (8)) [31].

$$\Gamma = cD_{total} \tag{6}$$

$$\Gamma = cD_{\text{total}}^{\text{b}} \tag{7}$$

$$\Gamma = \text{c}\, e^{bD_{total}} \tag{8}$$

where c and b are empirical constants, and Γ is any quantitative critical material performance characteristic such as specimen thickness, stiffness, toughness, etc. In this study, the linear response (equation (6)) has been applied in the UV simulation assuming that the damage characteristic, Γ, is represented by changes to specimen thickness by UV degradation on unit area. Therefore, Γ becomes $H_i - H_f$ in equation (9).

$$H_f = H_i - c\, D_{total} \tag{9}$$

where H_i and H_f are the initial and final specimen thicknesses

before and after UV exposure, respectively.

Polymer surfaces can be highly irregular. Especially in the case of PMCs, surface roughness can be significant and increased by the presence of surface glass fibers [1]. For simplicity, sinusoidal surface shapes have been assumed in this work. The numerical differentiation method has been adopted to simulate the degradation of a surface as a function of UV exposure. In order to find a relationship between the depth changes and the exposure time (dy/dt), we have expressed the depth change rate of a surface profile as a linear function of its slope and a coefficient, α, (equation (10)). Also, by substituting equations (4), (5) and (9) and $dy/dx=tan\ \theta$ into (10), we can find the correlation between 'α' and the coefficient 'c' as shown in equation (11). For any point, x_i, along the surface, θ in equation (5) can be calculated from dy/dx. Then the irradiation E_o on this inclined surface can be determined from the same equation.

$$\frac{dy}{dt} = \alpha \frac{\mathrm{dy}}{\mathrm{dx}} \tag{10}$$

$$\alpha = -c \cdot \phi \cdot I_o \cdot \frac{cos\theta}{tan\theta} \tag{11}$$

In order to solve equation (11) in MATLAB, firstly, a symmetric, sinusoidal curve was evenly divided into a number of elements with a constant length dx. The forward difference and backward difference methods were used to calculate the slope of the first and the last nodes by equations (12) and (13), respectively. The derivatives of the remaining nodes were computed by the centered difference scheme (equation (14)) to improve the numerical accuracy. Then, the lengths of all segments were computed from the slopes obtained from the previous steps. Finally, the irradiation distributions were determined from the irradiation amounts for all segments (computed by equation (5)) divided by the length of the segments.

$$y'(x_i) = \frac{y(x_{i+1}) - y(x_i)}{\Delta x} \tag{12}$$

$$y'(x_i) = \frac{y(x_i) - y(x_{i-1})}{\Delta x} \tag{13}$$

$$y'(x_i) = \frac{y(x_{i+1}) - y(x_{i-1})}{2\Delta x} \tag{14}$$

Since the relationship between UV damage to a polymer material and a radiation dosage has been defined as a linear function through equation (6), we can update the depth function y(x) by subtracting a correction term during each step (equation (15)). Furthermore, this iteration can continue with a certain amount of time to eventually reach a final result.

$$y(x_i, t + dt) = y(x_i, t) - aE(x_i, t)dt \tag{15}$$

For the orthogonal angle between UV light and a surface, there is a maximum UV irradiation associated with the maximum degradation rate. This is the reason why at the peaks and the valleys of the sinusoidal surface the degradation rates are at a maximum while those at the locations where the angle of inclination is 45° are at a minimum.

3. Experimental estimation of UV damage parameters

The UV degradation model presented in the previous section and in section 4 assumed that the polymer surface material damaged by UV is removed layer by layer reducing the thickness of the specimen with time. It also assumed that the rate of degradation (or the efficiency of UV damage formation) depended on the "c" parameter, which linearly relates the degradation rate to a dose of radiation (D_{total} in equations (4) and (6)) necessary to damage a small critical volume of the surface material. If this condition is satisfied, the small critical volume is immediately removed numerically from the surface without a trace. This can be accomplished relatively easily numerically. Physically, however, this is a much more complicated process. If the critical volume absorbs a required dose of radiation, then the volume would have to be physically removed from the surface. Even on perpendicular surfaces, most UV generated polymer particles do not fall off and tend to stay on the surface by adhesion [1,2]. If they are sufficiently large, they can be removed quite efficiently by slowly moving water [2]. In the absence of water, the particles would stay on the surface, protect the underlying virgin polymer material against UV, and significantly slow down the rate of degradation. It can also be assumed that after receiving a critical dose of UV radiation small volumes of the surface material, are "removed" by evaporation (volatiles) or by shrinkage, especially if a UV test is performed at elevated temperature. Shrinkage and evaporation could be occurring independently from the volume removal by micro particles, or in conjunction. In this section, we are showing how to handle the "perfect removal" of the critically damaged surface material by measuring the mass loss of a UV exposed specimen. If the mass loss is significant, the rate of degradation, c, can be estimated and related linearly through equation (6) to a change in specimen thickness. However, if the mass loss is small, then the rate of degradation would have to be estimated differently, for example, by directly measuring changes in specimen thickness. This much more accurate approach is demonstrated in section 5.

In Ref. 1 individual and combined UV radiation and water condensation aging tests were conducted in an environmental aging chamber on a unidirectional glass fiber/epoxy composite with an area fraction of exposed fibers of about 50.1%. The UV radiation tests were carried out for 1000 h with the UV wavelengths ranging from 300 to 400 nm at 80 °C. An irradiance level of 1.50 W/m^2 at 340 nm was chosen. The test temperatures under UV and water were lower than the glass transition temperatures, Tg, of the composite, which was above 120 °C. The relative humidity (RH) was 3 ± 2%. In addition to using the already published data for the composite, UV aging tests were also conducted in this work on neat relatively flat PVC samples under identical conditions to evaluate their mass losses under UV and temperature separately. Tg of the tested PVC was about 80 °C. The composite and PVC specimens had the same dimensions. This allowed us to estimate the level of degradation of the wavy composite samples and the flat PVC samples, and to determine the c values for equation (6) from two different polymeric materials, separately.

The average mass changes of the epoxy based polymer composite and the PVC samples under UV radiation and at 80 °C alone for 1000 h are shown in Fig. 2a and b. The mass losses seem to decelerate with time in both cases. This can be attributed to the reductions in the amounts of available volatiles with time under heat and UV and heat alone. It can also be attributed to the presence of polymer particles adhered to the surface and exposed glass fibers under UV preventing further degradation of the material underneath (Fig. 1a). The same effect was observed for the PVC after radiation, which by the way, lost more mass after 1000 h. The fact that the PVC samples were affected by UV more could be explained by their, perhaps lower resistance to UV radiation but also by a much larger surface area of the polymer exposed to UV in PVC (100%) vs. about 50% for the composite. The percent exposed area of the polymer in the composite was determined from the experimentally measured fiber surface area exposures [34].

Under 80 °C alone both materials lost mass because of the

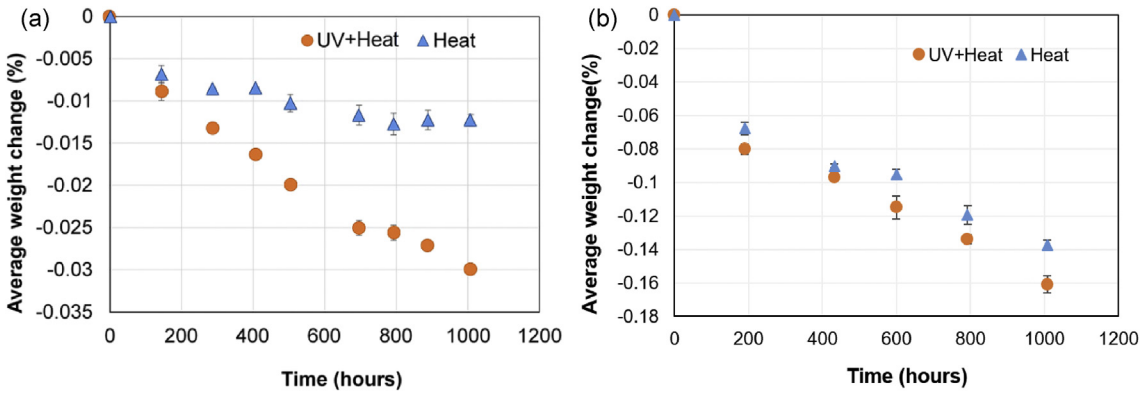

Fig. 2. Average weight changes of epoxy polymer composite (a) and PVC (b) samples at 80 °C with and without UV.

evaporation of volatile organic compounds. It appears that more volatiles were lost under temperature alone from the PVC samples than from the composite. As seen in Fig. 2, the average weight loss of the composite samples caused by the thermal condition was almost half of the total weight loss under UV radiation at the same temperature. The weight loss by temperature of the PVC samples was stronger in comparison with the UV caused loses.

It is stipulated here that the mass loss caused by the removal of a "solid" UV generated substance from the composite and the polymer is the result of the mass change under UV minus the mass change under the thermal condition. Therefore, linear curve fitting was used to obtain the estimated value of "c" in equation (6) for the two materials from the difference in the mass losses by UV and temperature (Fig. 5). The c values are the slopes of the curves in Fig. 3. The slopes were found to be close but different. For the modeling analysis, the c value was considered to be 2×10^{-5}. It is also assumed that the changes in specimen thickness are directly proportional to the amount of degradation and are linearly dependent on time. Therefore, the changes in specimen thickness can now be related to time for the assumed E_o and Φ values according to equations (4) and (16).

$$H_f = H_i - 2 \times 10^{-5} D_{total} \tag{16}$$

4. Simulations of UV radiation on polymeric surfaces

The UV degradation model developed in this work required certain physical constants as the input parameters in the subsequent numerical simulations of UV damage. Quantum yield, Φ, was taken from literature [26] whereas the others followed the experiments described above. All used physical constants are listed in Table 1.

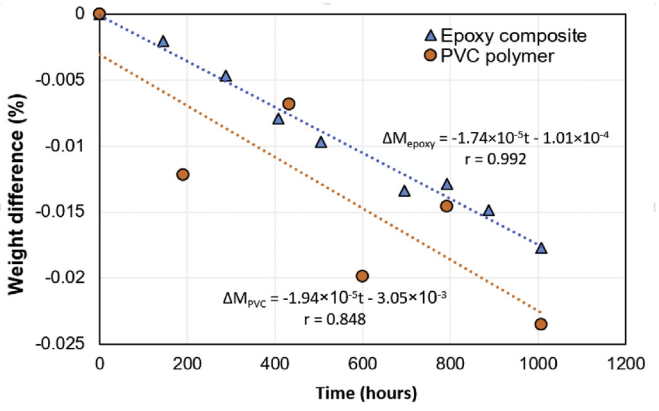

Fig. 3. Estimated weight changes of epoxy composite and PVC polymer samples by UV radiation condition for 1000 h after extracting the 80 °C heat effect in Fig. 2.

4.1. Radiation angle effect on flat surfaces

If we assume that a flat polymer sample with an initial thickness of 1 mm is subjected to UV in two directions (perpendicular and at 45) for 1000 h, the thickness of the sample will change for the two exposure directions according to the simulated data shown in Fig. 4. As expected the thickness reduction of the samples exposed perpendicularly is by an expected factor of 1/cos (45).

4.2. UV radiation damage of sinusoidal surfaces

The stages of polymer degradation from an initially sinusoidal surface, based on equation (15) are shown in Fig. 5. A much large value of parameter 'a' in Equation (15) was used (0.01) to accelerate the rates of numerical photodegradation for an arbitrarily chosen polymer material. In Fig. 5 the reduction in specimen thickness of the polymer is shown along the Y direction in arbitrary units. When the angle between the UV light and the surface is 90°, there is a maximum UV irradiation associated with the maximum degradation rate. That is the reason why the degradation rates at the peaks and the valleys of the surface are much greater than those at the locations where the angle of inclination is around 45°. In a more general case the surface profile could be $B \cdot \sin(x)$ where B is an arbitrary coefficient related to the surface roughness, the maximum angle of inclination could be less than or greater than 45°. It can be noticed in Fig. 6 that initially the tops and bottoms of the surface exhibit higher degradation rates than those at the other locations. However, when a sharp bottom is formed at the valley, the degradation rate in this location starts to decline, whereas the degradation rate on the top remains the same. As a result, the inclination will gradually diminish, and a flat shape will eventually become

Table 1
Physical parameters required for the UV radiation simulations.

Parameter	Value
Sensitive wavelength, λ	300–340 nm
Radiation intensity, Eo	1.5 W/m^2
Quantum yield Φ	10^{-4} [26]
Exposure time, t	1000 h (3.6×10^6s)
Exposure area	3.25×10^{-3} m^2

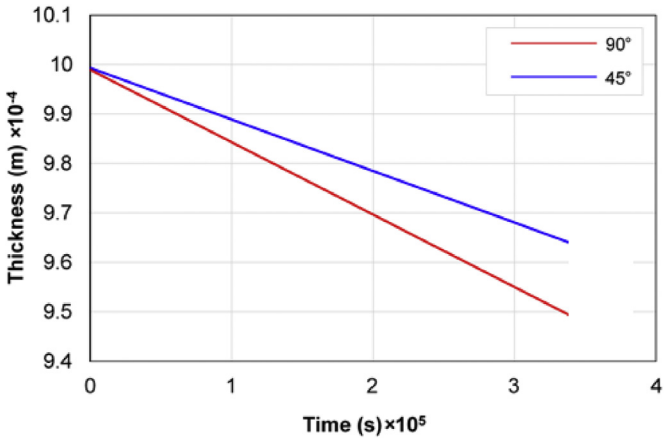

Fig. 4. Thickness reduction rates with respect to time under different radiation angles (in degree).

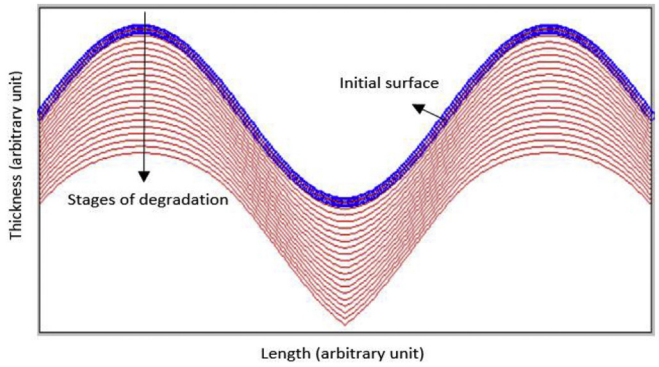

Fig. 5. Initial stages of UV degradation of a sinusoidal polymeric surface subjected to UV at 90°.

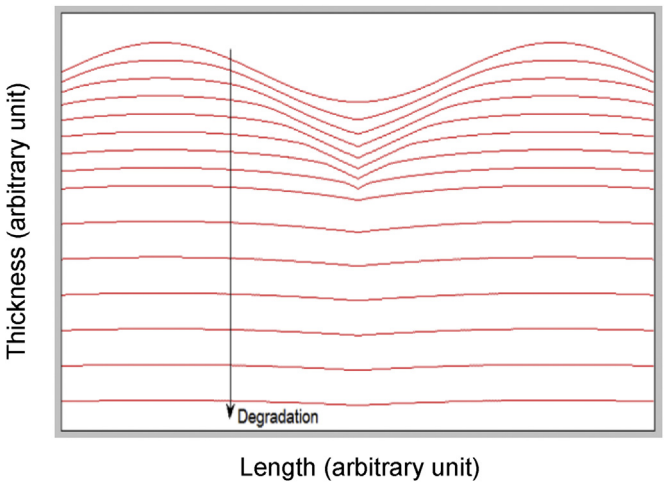

Fig. 6. Complete UV degradation of a sinusoidal polymeric surface subjected to UV at 90°.

dominant on the entire surface (Fig. 6).

The degradation rates at different locations of the sinusoidal surface are functions of time, as shown in Fig. 7. The peak locations are subjected to constant degradation rates because the radiation is directed perpendicularly to the surface at this location and there is no angle change during exposure. At a location where the angle

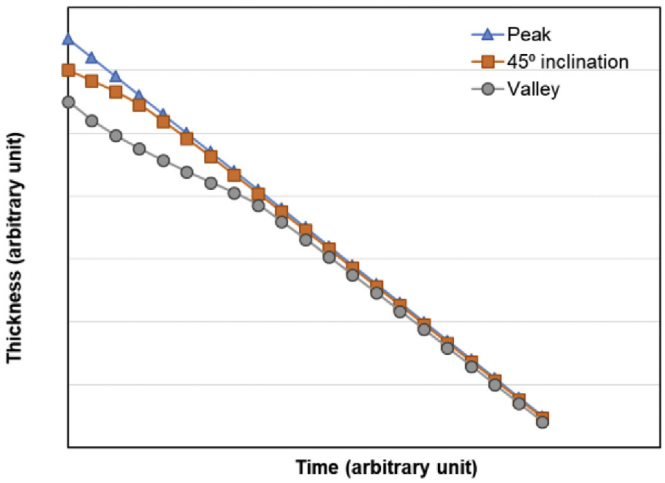

Fig. 7. Thickness degradation at three different locations of the sinusoidal surface.

between the surface and UV is 45°, the degradation slowly accelerates as the slope of the surface becomes smaller. At the bottom of the valley the degradation rate is reduced at the beginning, and then increases. There is a maximum, initial degradation rate that is the same as that at the peaks because of the 0° incident angle. However, when the surface profile is approaching a straight line, the degradation rate will slow down and become equal to the rate at 45°. After that, due to the slowed degradation rate at the valleys the sinusoidal surface will become flat and the degradation rate of the valleys will increasingly approach the rate at the peaks again.

One problem which has been encountered in the numerical simulation of UV degradation using MATLAB is that the result could not converge in some situations, as shown in Fig. 8. It was observed that there were very small errors in the initial iteration (~10^{-16}). After several iterations, however, the errors accumulated and became more and more significant, eventually leading to a divergent solution. It has been found that it is important to keep the ratio of the number of time steps to the number of nodes above a certain threshold to avoid numerical oscillations in the solution. In this research the critical number was 50.

It should be pointed out that the explicit finite difference method has been used to solve equations (11)–(14). This method differs from the implicit method where the solution is unconditionally stable. The numerical issues encountered in this work are analogous to those in the transient heat conduction simulation, in which there exists a critical Fourier number (0.5 in the one-dimensional problem, for example) leading to a divergent solution [35]. This implies that there could also exist a critical value in the current problem that determines the numerical stability. It has also been found in this work that it is a good strategy to employ a symmetric surface profile to avoid possible numerical problems in the UV damage simulation since the numerical errors tend to cancel out in the presence of symmetrical domains.

5. Verification of the UV radiation model

In this part of the study, the UV degradation model was experimentally verified by monitoring the local changes in the surface topographies of neat epoxy specimens subjected to UV. An unpigmented epoxy resin and a hardener, both supplied by Buehler Inc., were used to fabricate epoxy specimens according to manufacturer's specifications for UV exposure. A Q-LAB accelerated weathering tester model QUV/spray with an irradiance level of 1.5 W/m^2 at 340 nm wavelength was used in the UV testing. The

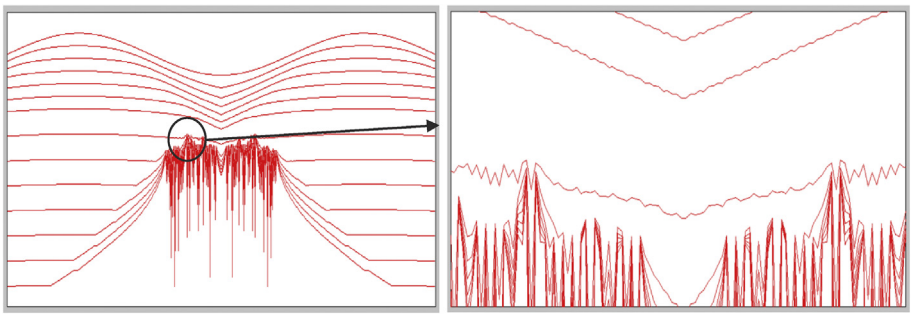

Fig. 8. Examples of severe oscillations in the solution caused by the numerical instability.

Table 2
Comparison of average surface roughness of unexposed and exposed to UV epoxy surfaces after 1000 h.

Surface Conditions	R_q (μm)		% change
	Unexposed	UV exposed	
As supplied	1.6 ± 0.2	1.4 ± 0.1	12.5

tests were carried out for 1000 h at 80 °C and the relative humidity was 3 ± 2% dry. Subsequently, the samples were evaluated for their surface roughness as a function of time both on their unexposed and exposed surfaces. The roughness was determined by the root mean square roughness (R_q), also known as RMS. using equation (17). A total of 15 surface profiles were collected using a Keyence white light interference microscope (wide-area 3D measurement system-VR-3100 Series). The results from the tests are listed in Table 2. In addition, two examples of the virgin and exposed to UV surfaces are shown in Fig. 9. It can be noticed in Table 2 that the average roughness of the specimens was reduced by 12.5% after 1000 h of UV exposure. Using the *t*-test approach, it was also determined that the roughness data obtained before and after the UV exposures were statistically different. This thus supports the UV planarization effect observed numerically.

$$R_q = RMS = \sqrt{\frac{1}{n}\sum_{i=1}^{n} y_i^2} \tag{17}$$

The UV planarization effect on irregular polymeric surfaces can also be observed in Fig. 10, which contains two surface profiles obtained before and after UV exposure for 1000 h. It has been observed in this study that the UV planarization mechanism is mainly associated with a significant reduction of surface amplitudes and that the peaks are more affected than the valleys (see Fig. 10). This resulted in a reduction in the specimen thickness, $\Delta H = H_i - H_f$, with time, t. The effectiveness of UV degradation, c, can be determined by $-\Delta H/D_{total}$. For the epoxy specimens, the thickness was reduced by 9.4 ± 1.7 μm in 1000 h and the effectiveness was estimated to be -1.12×10^{-5}.

It should be noted here that the "*c*" parameter obtained by the direct thickness reduction estimations in the epoxy specimens was much smaller than those obtained by the mass change evaluation, and then from the indirect thickness estimation, for the

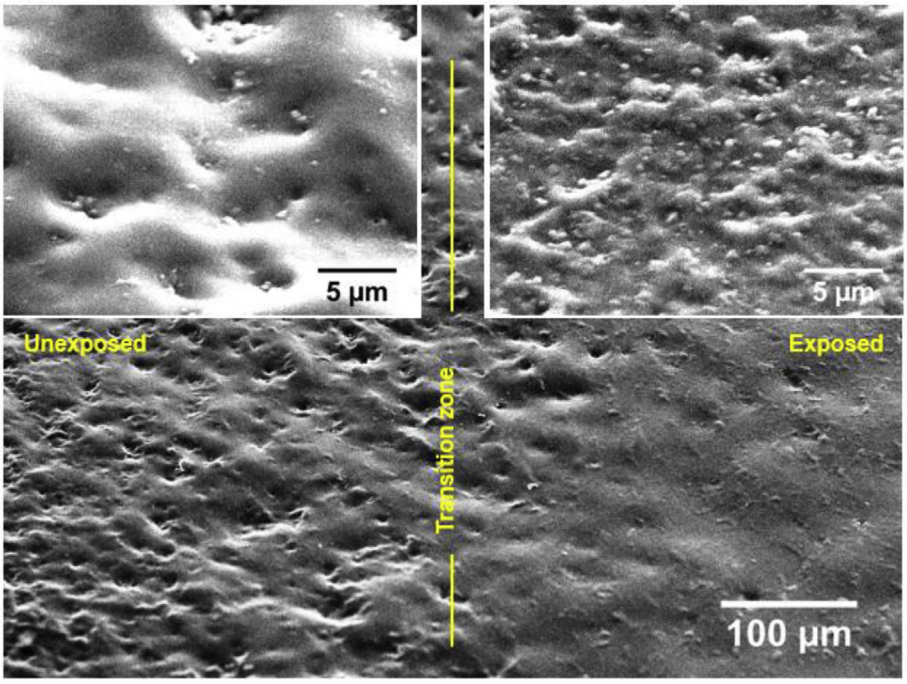

Fig. 9. Surface topographies of unexposed (left) and UV exposed (right) for 1000 h surfaces of the epoxy specimens. Inserts show magnified SEM images of their surface topographies.

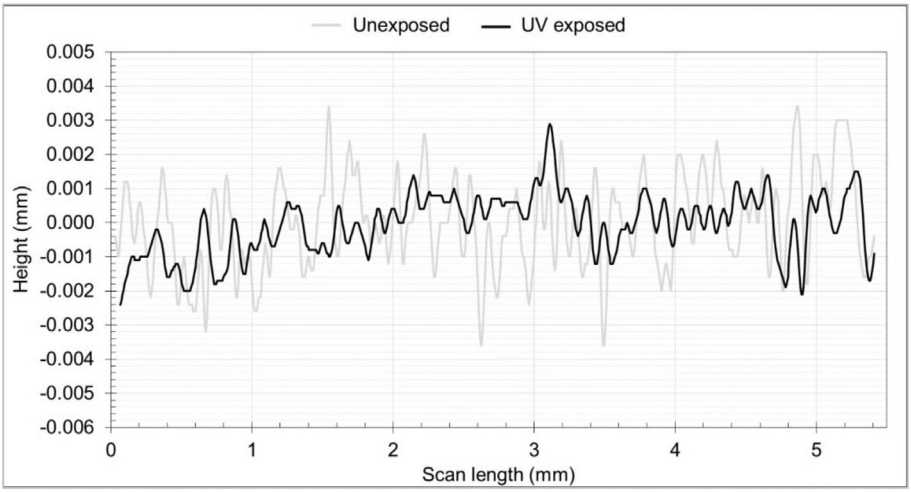

Fig. 10. Representation of planarization effect after UV exposure.

unidirectional glass fiber epoxy composite and the PVC samples described in section 3. For the neat epoxy specimens, the c value was found to be approximately 10 times smaller than for the other two materials. This can be attributed to a much better resistance of the epoxy to UV degradation, since, contrary to the epoxy composite and PVC samples, the neat epoxy specimens developed multiple but much smaller particles after 1000 h (Fig. 9, upper right corner) and its UV surface damage appeared to be in its initial stages. Therefore, the UV degradation of the neat epoxy specimens must have been predominantly associated with the thickness reduction by the evaporation of volatiles and shrinkage and by the initial formation of very small particles. It must also be added at this point that the c estimations from the mass loss of badly damaged samples might not be accurate leading to severe underestimations of degradation rates due to the presence of the particles still left on the surface. The particles left on the surface will also create problems in the direct measurements of surface profiles and specimen thickness estimations using the technique presented in this section. This approach, however, is very accurate for the monitoring of the very initial stages of UV degradation in polymers and polymer matrix composites.

6. Summary observations and conclusions

It has been found in this work that UV degradation of polymeric surfaces is strongly dependent on UV wavelength, intensity and exposure time. It is also shown that UV intensity and inclinations determine the local degradation rates of the material which can be numerically simulated from the global degradation rates for a material determined experimentally. The finite difference method was successfully applied in the UV radiation simulation to study the evolution of the sinusoidal surface due to the material degradation under UV exposure. The simulation parameters were appropriately defined to avoid numerical instabilities in the solution. Through the numerical simulations it is concluded that the initial irregular, sinusoidal surface of the material will be eventually degraded to a flat surface under a long period of exposure to UV radiation regardless of the irradiation angle. Although the simulations were performed in the setting of sinusoidal surfaces, the methodology is equally applicable to any irregular surfaces. The UV planarization effect on irregular polymeric surfaces observed numerically was finally experimentally verified in this work by the UV testing of neat epoxy specimens at elevated temperature. The surface roughness of the specimens was reduced by about 12.5% after 1000 h of UV exposure.

Acknowledgments

This work was funded by the National Science Foundation I/UCRC Center for Novel High Voltage Materials and Structures under #IIP 1362135 and by the NSF Grant Opportunities for Academic Liaison with Industry program under #CMMI-123252.

References

[1] T. Lu, E. Solis-Ramos, Yun-Bo Yi, M. Kumosa, Synergistic environmental degradation of glass reinforced polymer composites, Polym. Degrad. Stabil. 131 (2016) 1–8.
[2] T. Lu, E. Solis-Ramos, Y. Yi, M. Kumosa, Particle removal mechanisms in synergistic aging of polymers and glass reinforced polymer composites under combined UV and water, Compos. Sci. Technol. 153 (2017) 273–281.
[3] H.A. Al-Turaif, Surface morphology and chemistry of epoxy-based coatings after exposure to ultraviolet radiation, Prog. Org. Coating 76 (4) (2013) 677–681.
[4] F. Dupuis, A.U. Perrin, J. Torres, L. Habas, J. Belec, Chailan. Photo-oxidative degradation behavior of linseed oil based epoxy resin, Polym. Degrad. Stabil. 135 (2017) 73–84.
[5] S. Commereuc, H. Askanian, V. Verney, A. Celli, P. Marchese, C. Berti, About the end life of novel aliphatic and aliphatic-aromatic (co)polyesters after UV-weathering: structure/degradability relationships, Polym. Degrad. Stabil. 98 (7) (2013) 1321–1328.
[6] A. Ghasemi-Kahrizsangi, H. Shariatpanahi, J. Neshati, E. Akbarinezhad, Degradation of modified carbon black/epoxy nanocomposite coatings under ultraviolet exposure, Appl. Surf. Sci. 353 (2015) 530–539.
[7] Z. Chen, L. Zheng, Q. Jin, X. Li, Durability study on glass fiber reinforced polymer soil nail via accelerated aging test and long-term field test, Polym. Compos. (2015) 1–11.
[8] P. Böer, L. Holliday, T.H.-K. Kang, Independent environmental effects on durability of fiber-reinforced polymer wraps in civil applications: a review, Construct. Build. Mater. 48 (2013) 360–370.
[9] G. Carra, V. Carvelli, Ageing of pultruded glass fibre reinforced polymer composites exposed to combined environmental agents, Compos. Struct. 108 (2014) 1019–1026.
[10] S. Hinderliter, Croll. Monte carlo approach to estimating the photodegradation of polymer coatings, J. Coating Technol. Res. 2 (6) (2005) 483–491.
[11] S.G. Croll, B.R. Hinderliter, S. Liu, Statistical approaches for predicting weathering degradation and service fife, Prog. Org. Coating 55 (2) (2006) 75–87.
[12] B. Hinderliter, S. Croll, Predicting coating failure using the central limit theorem and physical modeling, ECS Trans. 24 (1) (2010) 1–26.
[13] E. Yousif, R. Haddad, Photodegradation and photostabilization of polymers, especially polystyrene: review, SpringerPlus 2 (1) (2013) 398.
[14] T.T.X. Hang, N.T. Dung, T.A. Truc, N.T. Duong, B.V. Truoc, P.G. Vu, T. Hoang, D.T.M. Thanh, M. Olivier, Effect of silane modified nano ZnO on UV degradation of polyurethane coatings, Prog. Org. Coating 79 (2015) 68–74.
[15] H. Makki, K.N.S. Adema, E.A.J.F. Peters, J. Laven, L.G.J. van der Ven, R.A.T.M. van Benthem, G. de With, A simulation approach to study photo-degradation processes of polymeric coatings, Polym. Degrad. Stabil. 105 (2014) 68–79.

[16] V.C. Malshe, G. Waghoo, Weathering study of epoxy paints, Prog. Org. Coating 51 (4) (2004) 267–272.
[17] V.C. Malshe, G. Waghoo, Chalk resistant epoxy resins, Prog. Org. Coating 51 (3) (2004) 172–180.
[18] A. de Souza Rios, W.F. de Amorim Júnior, E.P. de Moura, E.P. de Deus, J.P. de Andrade Feitosa, Effects of accelerated aging on mechanical, thermal and morphological behavior of polyurethane/epoxy/fiberglass composites, Polym. Test. 50 (2016) 152–163.
[19] V.M. Karbhari, Durability of Composites for Civil Structural Applications, first ed., 2007. Abington Cambridge.
[20] G. Wypych, Handbook of UV Degradation and Stabilization, Toronto, 2011.
[21] Y. Hu, X. Li, A.W. Lang, Y. Zhang, S.R. Nutt, Water immersion aging of polydicyclopentadiene resin and glass fiber composites, Polym. Degrad. Stabil. 124 (2016) 35–42.
[22] J. Park, P. Shin, Z. Wang, D. Kwon, J. Choi, S. Lee, K.L. DeVries, The change in mechanical and interfacial properties of GF and CF reinforced epoxy composites after aging in NaCl solution, Compos. Sci. Technol. 122 (2016) 59–66.
[23] J. Wang, H. GangaRao, R. Liang, D. Zhou, W. Liu, Y. Fang, Durability of glass fiber-reinforced polymer composites under the combined effects of moisture and sustained loads, J. Reinforc. Plast. Compos. 34 (21) (2015) 1739–1754.
[24] M. Evans, A statistical degradation model for the service life prediction of aircraft coatings: with a comparison to an existing methodology, Polym. Test. 31 (1) (2012) 46–55.
[25] S.G. Croll, Application and limitations of current understanding to model failure modes in coatings, J. Coating Technol. Res. (2012) 15–27.
[26] S. Kiil, Model-based analysis of photoinitiated coating degradation under artificial exposure conditions, J. Coating Technol. Res. 9 (4) (2012) 375–398.
[27] B.G. Kumar, R.P. Singh, T. Nakamura, Degradation of carbon fiber-reinforced epoxy composites by ultraviolet radiation and condensation, J. Compos. Mater. 36 (2002) 2713–2721.
[28] D.E. Mouzakis, H. Zoga, C. Galiotis, Accelerated environmental ageing study of polyester/glass fiber reinforced composites (GFRPCs), Composites Part B 39 (2008) 467–475.
[29] C. Dubois, L. Monney, N. Bonenet, A. Chambaudet, Degradation of an epoxy-glass-fibre laminate under photo-oxidation/leaching complementary constraints, Composites Part A 30 (1999) 361–368.
[30] A. François-Heude, E. Richaud, E. Desnoux, X. Colin, Influence of temperature, UV-light wavelength and intensity on polypropylene photothermal oxidation, Polym. Degrad. Stabil. 100 (2014) 10–20.
[31] J.W. Martin, Quantitative characterization of spectral ultraviolet radiation-induced photodegradation in coating systems exposed in the laboratory and the field, Prog. Org. Coating 23 (1) (1993) 49–70.
[32] J.W. Martin, T. Nguyen, E. Byrd, B. Dickens, N. Embree, Relating laboratory and outdoor exposures of acrylic melamine coatings: I. Cumulative damage model and laboratory exposure apparatus, Polym. Degrad. Stabil. 75 (2002) 193–210.
[33] P. Incropera, D.P. Dewitt, T.L. Bergman, A.S. Lavine, Fundamentals of Heat and Mass Transfer, sixth ed., 2006. Hoboken.
[34] T. Lu, Degradation of High Voltage Glass Fiber-reinforced Polymer Matrix Composites by Aggressive Environmental Conditions, MS Thesis, University of Denver, Denver Colorado, August 2014.
[35] B. Carnahan, H.A. Luther, J.O. Wilkes, Applied Numerical Methods, New York, 1969.